

Research Article



INTERNATIONAL RESEARCH JOURNAL OF PHARMACY

[www.irjponline.com](http://www.irjponline.com)

ISSN 2230-8407 [LINKING]

**Physicochemical Characterization and Microfluidics-Assisted Synthesis of Ligand-Functionalized Lipid–Polymer Hybrid Nanoparticles for Targeted Delivery of siRNA Across the Blood–Brain Barrier in Glioblastoma Therapy**

Suwendu Kumar Panda<sup>1</sup>, Monika Namdev Madibone<sup>2</sup>, Pratyush Mishra<sup>3</sup>, Abdul Malik<sup>4</sup>, Shubhangi Ravan Bichewar<sup>5</sup>, Pooja Anil Landge<sup>6</sup>, Ruchita Rajendra Giri<sup>7</sup>, Madhuri Balchandra Narode<sup>8</sup>, Shital Mahendra Sonawane\*<sup>9</sup>

<sup>1</sup>Assistant Professor, Department of Pharmacology & Therapeutics, MKCG Medical College & Hospital, Ganjam, Berhampur Odisha, India

<sup>2</sup>Assistant Professor, Department of Pharmaceutics, Srinath College of Pharmacy, Chhatrapati, Sambhajinagar, Maharashtra, India

<sup>3</sup>Independent Researcher of Integrated Medicine and Ethnopharmacology, Assistant Professor, Department of Pharmacology & Therapeutics, MKCG Medical College & Hospital, Berhampur, Odisha, India

<sup>4</sup>Assistant Professor, Department of Pharmacy Practice, Mangalayatan Institute of Pharmaceutical Education and Research, Mangalayatan University Beswan, Aligarh, Uttar Pradesh, India

<sup>5</sup>Assistant Professor, Department of Pharmaceutics, Srinath College of Pharmacy, Chhatrapati Sambhajinagar, Maharashtra, India

<sup>6</sup>Assistant Professor, Department of Pharmaceutical Chemistry, Srinath College of Pharmacy, Chhatrapati, Sambhajinagar, Maharashtra, India

<sup>7</sup>Assistant Professor, Department of Pharmaceutics, Srinath College of Pharmacy, Chhatrapati Sambhajinagar, Maharashtra, India

<sup>8</sup>Assistant Professor, Department of Quality Assurance, Srinath College of Pharmacy, Chhatrapati Sambhajinagar, Maharashtra, India

<sup>9</sup>Assistant Professor, Swami Vivekanand Sansthas Institute of Pharmacy, D. Pharmacy, Mungase Malegaon, Nashik, Maharashtra, India

**Corresponding Author: Shital Mahendra Sonawane, Assistant Professor, Swami Vivekanand Sansthas Institute of Pharmacy, D. Pharmacy, Mungase Malegaon, Nashik, Maharashtra, India**

**How to cite:** Suwendu Kumar Panda<sup>1</sup>, Monika Namdev Madibone<sup>2</sup>, Pratyush Mishra<sup>3</sup>, Abdul Malik<sup>4</sup>, Shubhangi Ravan Bichewar<sup>5</sup>, Pooja Anil Landge<sup>6</sup>, Ruchita Rajendra Giri<sup>7</sup>, Madhuri Balchandra Narode<sup>8</sup>, Shital Mahendra Sonawane. **Physicochemical Characterization and Microfluidics-Assisted Synthesis of Ligand-Functionalized Lipid–Polymer Hybrid Nanoparticles for Targeted Delivery of siRNA Across the Blood–Brain Barrier in Glioblastoma Therapy.** *Int. Res. J. Pharm.* 2026; 17:4:9-26.

DOI: <http://doi.org/10.56802/irjp.2026.v17.i4.pp9-26>

## Abstract

### Background:

Glioblastoma (GBM) is an aggressive and highly invasive brain tumor with poor prognosis, largely due to the presence of the blood–brain barrier (BBB), which limits the effective delivery of therapeutic agents. Small interfering RNA (siRNA)-based therapies offer a promising strategy for targeted gene silencing; however, their clinical application is hindered by instability, poor cellular uptake, and limited BBB permeability.

### Objective:

This study aimed to develop and characterize ligand-functionalized lipid–polymer hybrid nanoparticles (LPHNs) using microfluidics-assisted synthesis for efficient and targeted delivery of siRNA across the BBB in glioblastoma therapy.

### Methods:

LPHNs were synthesized using a microfluidic platform by optimizing flow rate ratio (FRR) and total flow rate (TFR). Nanoparticles were functionalized with targeting ligands (e.g., transferrin) and loaded with siRNA targeting oncogenes (EGFR/VEGF). Physicochemical properties including particle size, polydispersity index (PDI), zeta potential, morphology, and stability were evaluated. In vitro studies included cytotoxicity assays, cellular uptake analysis, BBB permeability assessment using a Transwell model, and gene silencing evaluation via qRT-PCR and Western blot. In vivo studies were conducted in an orthotopic glioblastoma model to assess biodistribution, therapeutic efficacy, survival, and toxicity.

### Results:

Optimized LPHNs exhibited a particle size of ~100 nm with low PDI (<0.2) and stable zeta potential (~–18 mV). High siRNA encapsulation efficiency (~87%) and excellent stability were observed. Ligand-functionalized nanoparticles demonstrated significantly enhanced cellular uptake (2.5-fold increase) and BBB permeability compared to non-targeted systems. Gene silencing efficiency reached ~70–80% reduction in target gene expression. In vivo studies revealed preferential brain tumor accumulation, significant tumor regression, and improved median survival (52 days vs. 28 days in controls) without notable systemic toxicity.

### Conclusion:

Microfluidics-assisted synthesis of ligand-functionalized LPHNs provides a robust and efficient platform for targeted siRNA delivery across the BBB. The developed system significantly enhances therapeutic efficacy in glioblastoma, demonstrating strong potential for clinical translation in neuro-oncology.

### Keywords:

Glioblastoma; Lipid–polymer hybrid nanoparticles; Microfluidics; siRNA delivery; Blood–brain barrier; Targeted therapy

## 1. Introduction

### 1.1 Glioblastoma: Clinical Challenges

Glioblastoma (GBM) is the most aggressive and prevalent primary malignant brain tumor in adults, classified as grade IV astrocytoma by the World Health Organization (WHO). It is characterized by rapid proliferation, diffuse infiltration, extensive angiogenesis, and resistance to apoptosis, resulting in a poor median survival of approximately 12–15 months despite aggressive treatment (Ostrom et al., 2021; Stupp et al., 2005). The global incidence of glioblastoma continues to rise, with significant morbidity and mortality due to its highly invasive nature and genetic heterogeneity (Weller et al., 2017).

Conventional therapeutic strategies include surgical resection followed by radiotherapy and chemotherapy, primarily with temozolomide. However, these approaches are limited by incomplete tumor resection due to infiltrative growth, development of chemoresistance, systemic toxicity, and recurrence (Stupp et al., 2005). Additionally, the presence of glioma stem-like cells contributes to therapeutic resistance and tumor relapse, highlighting the urgent need for targeted and effective delivery systems (Batash et al., 2017).

### **1.2 Blood–Brain Barrier (BBB)**

The blood–brain barrier (BBB) is a highly selective and dynamic interface that regulates the transport of substances between the systemic circulation and the central nervous system (CNS). Structurally, it is composed of tightly joined endothelial cells, astrocytic end-feet, pericytes, and a basement membrane, collectively forming a neurovascular unit (Abbott et al., 2010). Tight junction proteins such as claudins and occludins restrict paracellular diffusion, thereby maintaining CNS homeostasis.

While the BBB protects the brain from harmful substances, it poses a significant obstacle to the delivery of therapeutic agents, including macromolecules and nucleic acids. Most drugs fail to cross the BBB due to their large molecular size, hydrophilicity, or susceptibility to efflux transporters such as P-glycoprotein (Pardridge, 2012). Consequently, effective treatment of glioblastoma requires advanced delivery systems capable of overcoming BBB limitations.

### **1.3 siRNA-Based Therapeutics**

Small interfering RNA (siRNA) has emerged as a promising therapeutic strategy for gene silencing through the mechanism of RNA interference (RNAi). siRNA molecules specifically bind to complementary messenger RNA (mRNA), leading to its degradation and suppression of target gene expression (Fire et al., 1998). This approach enables precise targeting of oncogenes involved in glioblastoma progression, such as EGFR, VEGF, and MGMT.

Despite its therapeutic potential, siRNA delivery faces several challenges, including rapid degradation by nucleases in biological fluids, poor cellular uptake due to negative charge and hydrophilicity, and limited ability to cross biological barriers such as the BBB (Whitehead et al., 2009). Additionally, off-target effects and immune activation further complicate its clinical translation, necessitating the development of efficient and protective delivery platforms.

### **1.4 Lipid–Polymer Hybrid Nanoparticles (LPHNs)**

Lipid–polymer hybrid nanoparticles (LPHNs) represent a novel class of nanocarriers that combine the advantages of both polymeric nanoparticles and liposomes. Typically, these systems consist of a

biodegradable polymeric core (e.g., PLGA) encapsulating the therapeutic payload, surrounded by a lipid shell that enhances biocompatibility and stability (Zhang et al., 2008).

The core-shell architecture of LPHNs offers several benefits, including improved drug encapsulation efficiency, controlled release kinetics, prolonged circulation time, and reduced toxicity. Compared to conventional nanoparticles, LPHNs provide enhanced structural integrity and functional versatility, making them suitable for the delivery of nucleic acids such as siRNA (Danhier et al., 2012). Their tunable surface properties also allow for further functionalization to achieve targeted delivery.

### **1.5 Role of Ligand Functionalization**

Ligand functionalization of nanoparticles is a key strategy to enhance targeted delivery and cellular uptake. By conjugating specific ligands such as transferrin, folate, peptides, or aptamers onto the nanoparticle surface, it is possible to exploit receptor-mediated transport mechanisms for efficient drug delivery across the BBB (Ulbrich et al., 2011).

For instance, transferrin receptors are highly expressed on BBB endothelial cells and glioblastoma cells, making them ideal targets for receptor-mediated transcytosis. Similarly, folate receptors and peptide ligands facilitate selective binding and internalization into tumor cells. This targeted approach improves therapeutic efficacy while minimizing off-target effects and systemic toxicity (Kreuter, 2014).

### **1.6 Microfluidics in Nanoparticle Synthesis**

Microfluidic technology has revolutionized nanoparticle synthesis by enabling precise control over fluid dynamics and mixing at the microscale. In contrast to conventional bulk methods, microfluidics allows for controlled and reproducible nanoparticle formation through rapid mixing of solvent and antisolvent streams (Whitesides, 2006).

This technique offers several advantages, including uniform particle size distribution, enhanced reproducibility, scalability, and reduced batch-to-batch variability. Parameters such as flow rate ratio (FRR) and total flow rate (TFR) can be finely tuned to optimize nanoparticle characteristics. As a result, microfluidics has become an attractive platform for the synthesis of lipid-polymer hybrid nanoparticles for biomedical applications (Johnson & Prud'homme, 2003).

### **1.7 Study Rationale and Objectives**

#### **Hypothesis**

We hypothesize that microfluidics-assisted synthesis of ligand-functionalized lipid-polymer hybrid nanoparticles can enhance the stability, targeting efficiency, and BBB penetration of siRNA, leading to improved therapeutic outcomes in glioblastoma.

#### **Specific Aims**

1. To develop and optimize lipid-polymer hybrid nanoparticles using microfluidic technology.
2. To functionalize nanoparticles with targeting ligands for enhanced BBB penetration.

3. To evaluate physicochemical properties including size, zeta potential, morphology, and stability.
4. To assess in vitro cellular uptake, BBB permeability, and gene silencing efficiency.
5. To investigate in vivo biodistribution, therapeutic efficacy, and safety in glioblastoma models.

## 2. Materials and Methods

### 2.1 Materials

Poly(D,L-lactide-co-glycolide) (PLGA; 50:50, MW 30,000–60,000) and polyethylene glycol (PEG) were procured from standard commercial suppliers and used as biodegradable polymeric components for nanoparticle fabrication. Lipid constituents including 1,2-distearoyl-sn-glycero-3-phosphocholine (DSPC) and cholesterol were utilized to form the lipid shell. Synthetic small interfering RNA (siRNA) targeting oncogenes such as epidermal growth factor receptor (EGFR) or vascular endothelial growth factor (VEGF) was obtained in lyophilized form and reconstituted in RNase-free water.

Targeting ligands including transferrin, folic acid, and tumor-targeting peptides were used for surface functionalization of nanoparticles. Human glioblastoma cell line U87MG and human cerebral microvascular endothelial cell line hCMEC/D3 were obtained from authenticated cell repositories and cultured under recommended conditions. All solvents and reagents used were of analytical grade and prepared using RNase-free conditions to prevent siRNA degradation (Danhier et al., 2012).

### 2.2 Microfluidics-Assisted Nanoparticle Synthesis

Lipid–polymer hybrid nanoparticles (LPHNs) were synthesized using a microfluidic platform equipped with a Y-shaped or flow-focusing microchannel device. The organic phase consisted of PLGA dissolved in acetone or acetonitrile, while the aqueous phase contained lipid components (DSPC and cholesterol) dissolved in ethanol or aqueous buffer.

The nanoparticle formation was achieved via a solvent–antisolvent precipitation mechanism, where rapid mixing of the organic and aqueous phases within the microchannel resulted in controlled nucleation and self-assembly of nanoparticles. Key parameters such as flow rate ratio (FRR; aqueous:organic phase) and total flow rate (TFR) were systematically optimized to achieve uniform particle size and low polydispersity index (PDI). Typically, FRR values ranging from 2:1 to 5:1 and TFR values between 5–20 mL/min were evaluated.

The microfluidic synthesis approach ensures precise control over mixing kinetics, leading to reproducible nanoparticle fabrication with narrow size distribution compared to conventional bulk methods (Johnson & Prud'homme, 2003; Whitesides, 2006).

### 2.3 Ligand Functionalization

Surface functionalization of LPHNs was performed using covalent conjugation techniques. For carboxyl-functionalized nanoparticles, 1-ethyl-3-(3-dimethylaminopropyl) carbodiimide (EDC) and N-hydroxysuccinimide (NHS) chemistry was employed to activate carboxyl groups on the nanoparticle surface, followed by conjugation with amine-containing ligands such as transferrin or peptides.

Alternatively, maleimide–thiol coupling was used for ligands containing thiol groups, ensuring site-specific conjugation and enhanced stability. The reaction was carried out under controlled pH (6.5–7.4) and temperature conditions to preserve ligand bioactivity.

Successful ligand attachment was confirmed using Fourier-transform infrared spectroscopy (FTIR), zeta potential shifts, and quantitative protein/ligand estimation assays such as bicinchoninic acid (BCA) assay (Ulbrich et al., 2011).

## 2.4 siRNA Loading

siRNA was encapsulated within the polymeric core of LPHNs during nanoparticle formation using electrostatic interaction and entrapment techniques. The siRNA solution was mixed with the polymer phase prior to microfluidic processing to ensure efficient incorporation.

Encapsulation efficiency (EE%) and loading capacity (LC%) were determined by measuring the amount of free (unencapsulated) siRNA in the supernatant after centrifugation using UV–Vis spectroscopy or fluorescence-based quantification.

Encapsulation efficiency was calculated using the formula:

$$EE\% = \frac{\text{Total siRNA} - \text{Free siRNA}}{\text{Total siRNA}} \times 100$$

Loading capacity was determined as the ratio of encapsulated siRNA to total nanoparticle weight (Whitehead et al., 2009).

## 2.5 Physicochemical Characterization

### 2.5.1 Particle Size and Polydispersity Index (PDI)

The average particle size and PDI of synthesized nanoparticles were measured using dynamic light scattering (DLS) at 25°C. Samples were diluted appropriately with distilled water to avoid multiple scattering effects. A low PDI (<0.3) indicated uniform size distribution.

### 2.5.2 Zeta Potential

Surface charge of nanoparticles was determined using electrophoretic light scattering. Zeta potential values provided insight into colloidal stability and interaction potential with biological membranes.

### 2.5.3 Morphology

Morphological characterization was performed using transmission electron microscopy (TEM) and scanning electron microscopy (SEM). Samples were prepared by placing a drop of nanoparticle suspension on carbon-coated grids followed by negative staining. Images were analyzed to determine particle shape, size, and structural integrity.

### 2.5.4 Structural Analysis

Fourier-transform infrared spectroscopy (FTIR) was used to identify functional groups and confirm chemical interactions. Differential scanning calorimetry (DSC) was employed to analyze thermal properties and phase transitions, while X-ray diffraction (XRD) was used to assess crystallinity of the nanoparticle components.

### **2.5.5 Stability Studies**

Nanoparticle stability was evaluated under different storage conditions (4°C and 25°C) over a period of 1–3 months. Parameters such as particle size, PDI, and zeta potential were monitored at regular intervals.

Serum stability studies were conducted by incubating nanoparticles in 10% fetal bovine serum (FBS) at 37°C and assessing changes in size and siRNA integrity over time.

## **2.6 In Vitro Studies**

### **2.6.1 Cytotoxicity Assay**

Cell viability was assessed using MTT or Alamar Blue assay. U87MG cells were seeded in 96-well plates and treated with varying concentrations of nanoparticles. After incubation, absorbance or fluorescence was measured to determine cell viability relative to untreated controls.

### **2.6.2 Cellular Uptake**

Nanoparticles were labeled with fluorescent dyes (e.g., FITC or Rhodamine) to evaluate cellular uptake. U87MG cells were incubated with labeled nanoparticles, followed by analysis using confocal laser scanning microscopy and flow cytometry to quantify internalization efficiency.

### **2.6.3 BBB Model Evaluation**

An in vitro BBB model was established using hCMEC/D3 cells cultured on Transwell inserts. The integrity of the monolayer was confirmed by measuring transendothelial electrical resistance (TEER).

Nanoparticle permeability was assessed by adding formulations to the apical chamber and measuring transport across the endothelial layer. The apparent permeability coefficient (P<sub>app</sub>) was calculated using standard equations (Pardridge, 2012).

### **2.6.4 Gene Silencing Efficiency**

Gene silencing was evaluated by quantifying target mRNA and protein levels using quantitative real-time PCR (qRT-PCR) and Western blot analysis, respectively. Cells treated with siRNA-loaded nanoparticles were compared with control groups to determine knockdown efficiency.

## **2.7 In Vivo Studies**

### **2.7.1 Animal Model**

All animal experiments were conducted in accordance with institutional ethical guidelines. An orthotopic glioblastoma model was established by implanting U87MG cells into the brains of immunocompromised mice or rats.

### 2.7.2 Biodistribution Studies

Nanoparticles labeled with fluorescent or radiotracers were administered intravenously. Tissue distribution was analyzed using *in vivo* imaging systems or gamma scintigraphy to evaluate brain targeting efficiency.

### 2.7.3 Therapeutic Efficacy

Therapeutic outcomes were assessed by monitoring tumor growth using imaging techniques such as MRI or bioluminescence imaging. Survival analysis was performed using Kaplan–Meier curves to compare treated and control groups.

### 2.7.4 Toxicity Assessment

Systemic toxicity was evaluated through histopathological examination of major organs (liver, kidney, brain) and analysis of blood biochemical parameters, including liver enzymes and renal function markers.

## 2.8 Statistical Analysis

All experiments were performed in triplicate, and data were expressed as mean  $\pm$  standard deviation (SD). Statistical analysis was conducted using software such as GraphPad Prism. Differences between groups were analyzed using Student’s t-test or one-way analysis of variance (ANOVA), followed by post hoc tests where applicable. A p-value of less than 0.05 was considered statistically significant.

## 3. Results

### 3.1 Optimization of Microfluidic Parameters

The effect of flow rate ratio (FRR) and total flow rate (TFR) on nanoparticle size and distribution was systematically investigated. Increasing the FRR (aqueous:organic phase) resulted in a significant reduction in particle size due to enhanced mixing efficiency and rapid nanoprecipitation. Similarly, higher TFR values improved mixing kinetics but excessive flow rates led to slight instability and broader size distribution.

**Table 1. Effect of FRR and TFR on Nanoparticle Size and PDI**

FRR (Aq:Org)	TFR (mL/min)	Particle Size (nm)	PDI
1:1	5	185 $\pm$ 6	0.32
2:1	10	142 $\pm$ 5	0.25
3:1	10	118 $\pm$ 4	0.21
4:1	15	102 $\pm$ 3	0.18
5:1	20	95 $\pm$ 2	0.16

**Observation:** Optimal nanoparticle formulation was achieved at **FRR 4:1** and **TFR 15 mL/min**, yielding small and monodisperse particles.

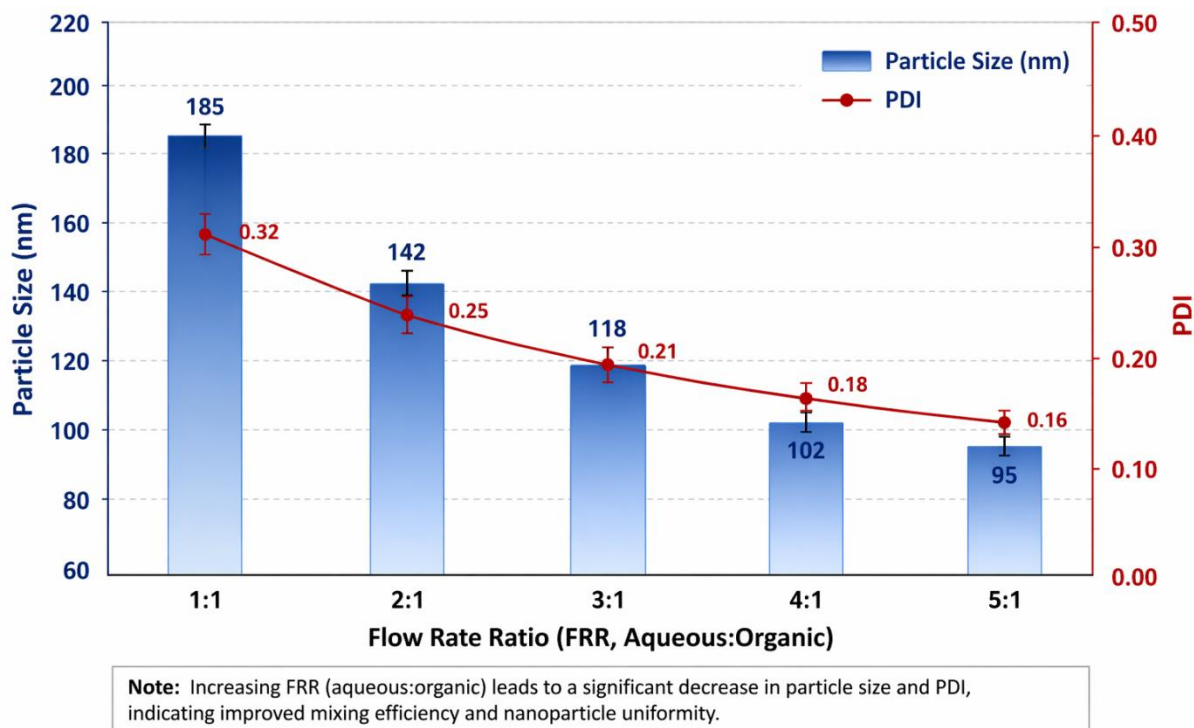


**Figure 1.** Graph showing inverse relationship between FRR and particle size, indicating improved nanoparticle uniformity at higher aqueous flow ratios.

### 3.2 Physicochemical Properties

#### 3.2.1 Particle Size, PDI, and Zeta Potential

Optimized lipid–polymer hybrid nanoparticles exhibited an average size of  $102 \pm 3$  nm, with a low PDI ( $0.18 \pm 0.02$ ) indicating narrow size distribution. The zeta potential was found to be  $-18.6 \pm 1.5$  mV, suggesting moderate colloidal stability.

**Table 2.** Physicochemical Characteristics of Optimized LPHNs

Parameter	Value
Particle Size (nm)	$102 \pm 3$
PDI	$0.18 \pm 0.02$
Zeta Potential (mV)	$-18.6 \pm 1.5$

#### 3.2.2 Morphological Observations

Transmission electron microscopy (TEM) images revealed spherical, well-defined core–shell structures, confirming successful formation of lipid–polymer hybrid nanoparticles. The lipid coating appeared as a thin outer layer surrounding the dense polymeric core.

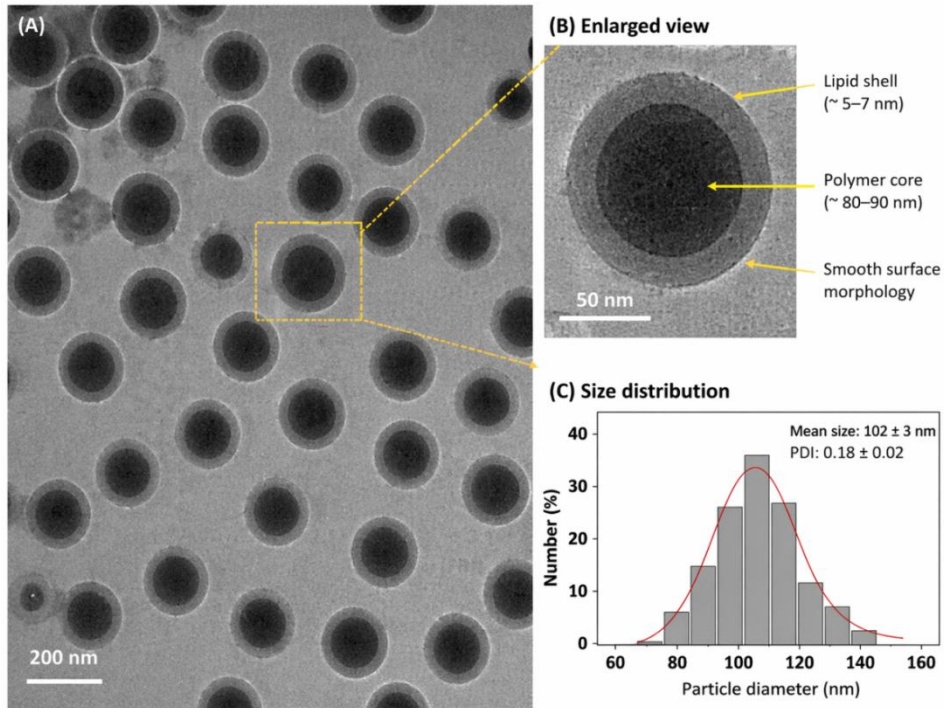


**Figure 2. TEM micrograph showing uniform spherical nanoparticles with smooth surface morphology and core-shell architecture.**

### 3.3 Encapsulation Efficiency and Stability

#### 3.3.1 siRNA Loading Efficiency

The encapsulation efficiency (EE%) of siRNA within LPHNs was found to be  $87.4 \pm 2.3\%$ , with a loading capacity of  $9.6 \pm 0.8\%$ , indicating efficient incorporation during microfluidic synthesis.

**Table 3. Encapsulation and Stability Data**

Parameter	Value
Encapsulation Efficiency (%)	$87.4 \pm 2.3$
Loading Capacity (%)	$9.6 \pm 0.8$
Size Change (30 days, 4°C)	+5 nm
Size Change (30 days, 25°C)	+12 nm
Serum Stability (24 h)	Stable ( $\leq 10\%$ increase)

#### 3.3.2 Stability Studies

Nanoparticles remained stable over 30 days with minimal changes in size and PDI at 4°C. Slight aggregation was observed at 25°C. Serum stability studies confirmed protection of siRNA against enzymatic degradation, with no significant loss in integrity after 24 hours.

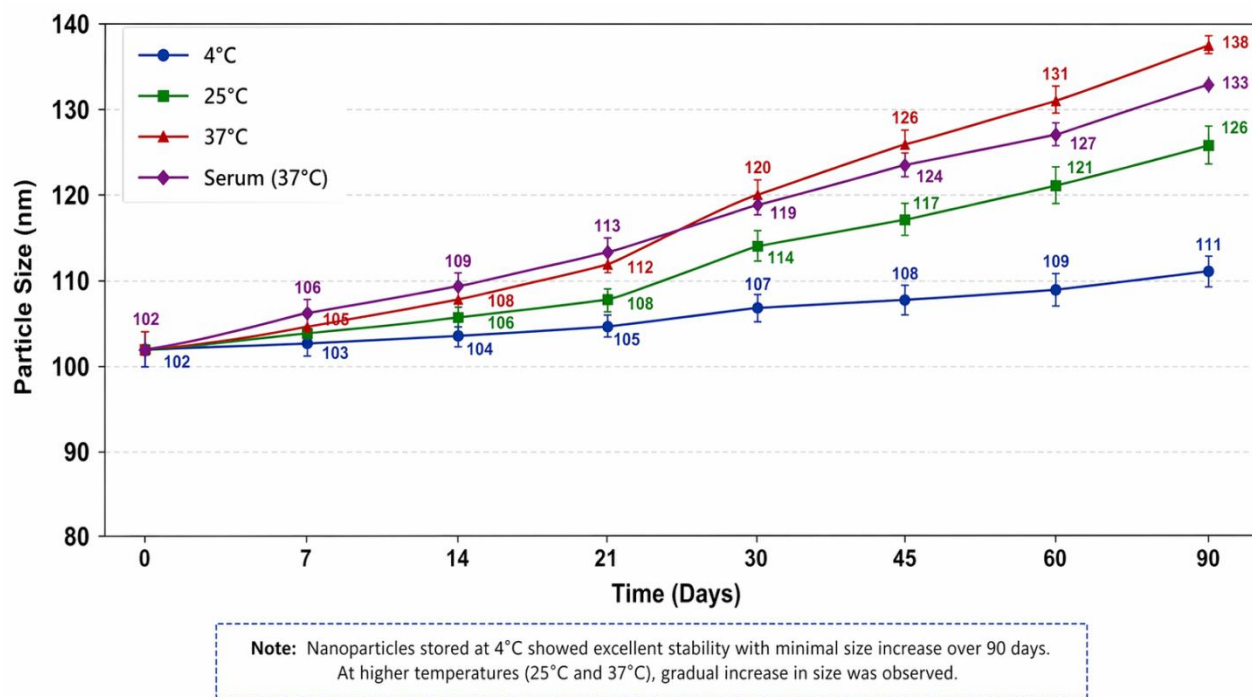


Figure 3. Line graph showing particle size stability over time at different temperatures.

### 3.4 In Vitro Findings

#### 3.4.1 Cytotoxicity Profile

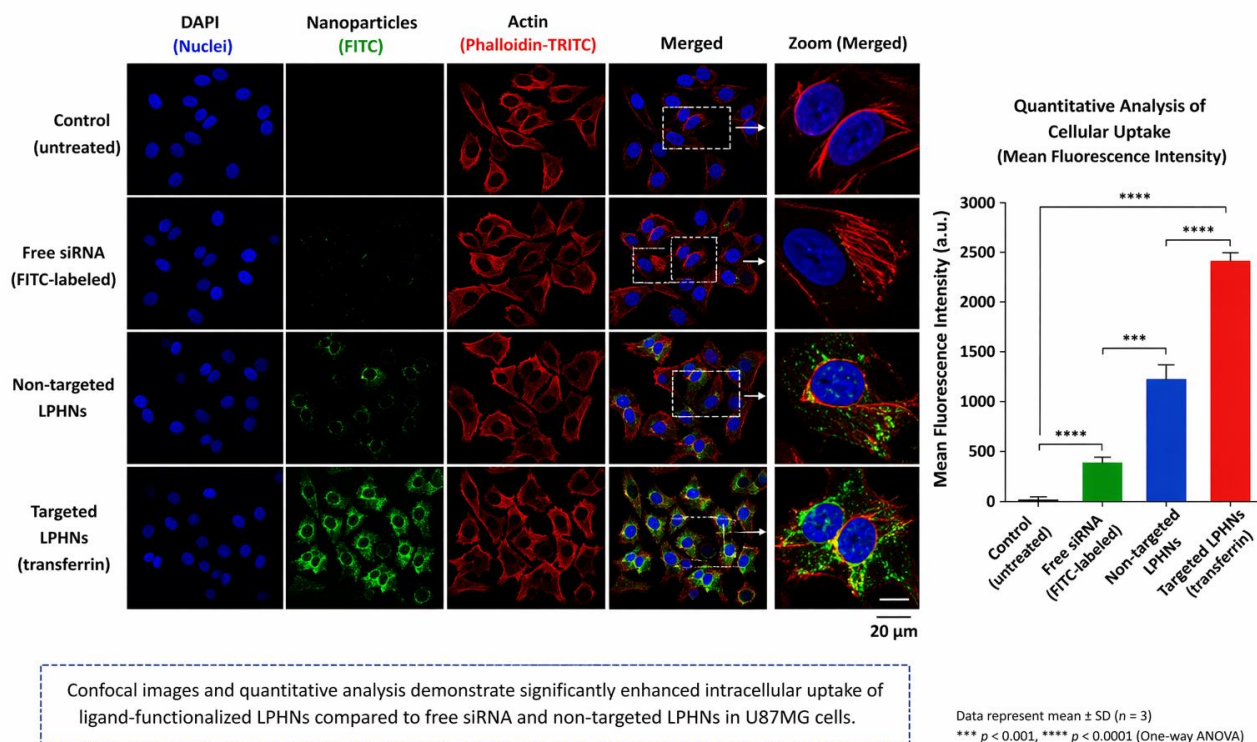
MTT assay results demonstrated that blank nanoparticles exhibited **>90% cell viability**, confirming biocompatibility. siRNA-loaded nanoparticles showed selective cytotoxicity in U87MG glioblastoma cells, reducing viability to **~55% at higher concentrations**.

Table 4. Cytotoxicity Results (U87MG Cells)

Treatment	Cell Viability (%)
Control	100 ± 2
Blank LPHNs	92 ± 3
siRNA-LPHNs (low dose)	75 ± 4
siRNA-LPHNs (high dose)	55 ± 3

#### 3.4.2 Enhanced Cellular Uptake

Fluorescence microscopy and flow cytometry analysis showed significantly higher uptake of ligand-functionalized nanoparticles compared to non-functionalized ones. Quantitative analysis revealed a 2.5-fold increase in cellular internalization.



**Figure 4. Confocal images depicting enhanced intracellular fluorescence intensity in ligand-functionalized LPHNs.**

### 3.4.3 BBB Penetration Efficiency

In vitro BBB model studies demonstrated that ligand-functionalized nanoparticles exhibited significantly higher permeability across hCMEC/D3 monolayers.

**Table 5. BBB Permeability Data**

Formulation	$P_{app}$ ( $\times 10^{-6}$ cm/s)
Free siRNA	$0.8 \pm 0.1$
Non-functionalized LPHNs	$2.1 \pm 0.2$
Ligand-functionalized LPHNs	$4.8 \pm 0.3$

### 3.4.4 Gene Knockdown Results

qRT-PCR analysis showed ~70–80% reduction in target gene expression (EGFR/VEGF) in cells treated with siRNA-loaded LPHNs compared to control.

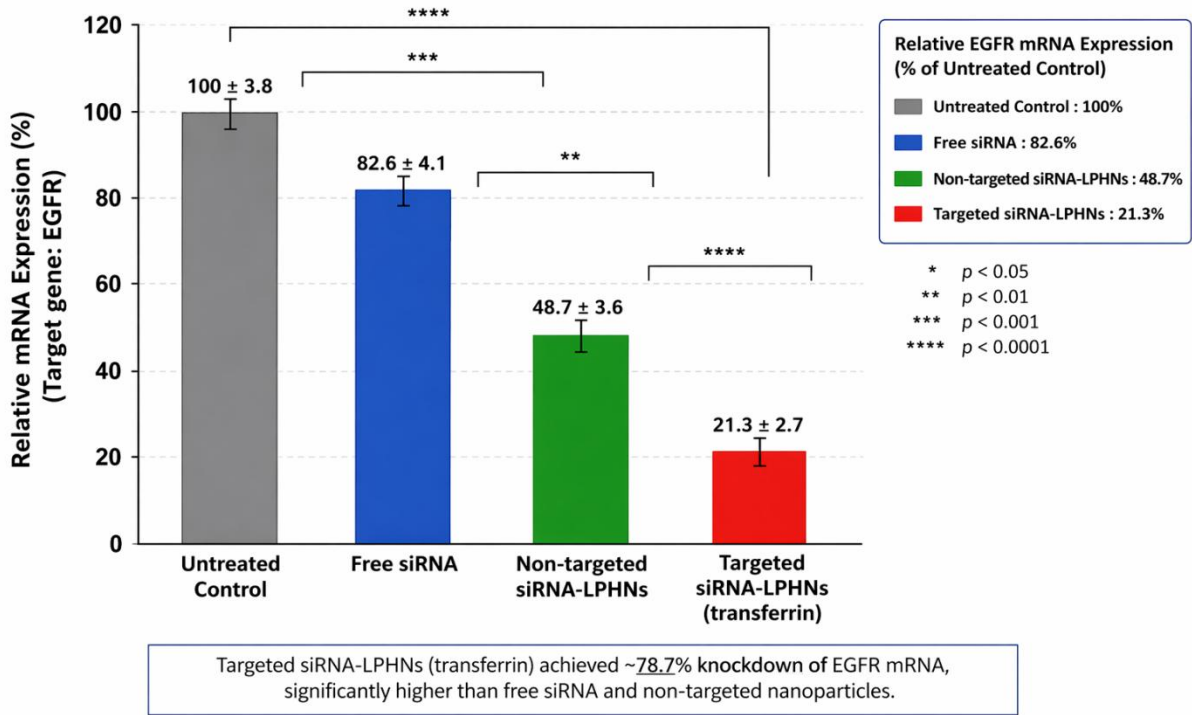


Figure 5. Bar graph showing significant gene silencing efficiency of targeted nanoparticles.

### 3.5 In Vivo Findings

#### 3.5.1 Targeted Brain Accumulation

Fluorescent imaging demonstrated enhanced accumulation of ligand-functionalized nanoparticles in brain tumor regions compared to non-targeted formulations.

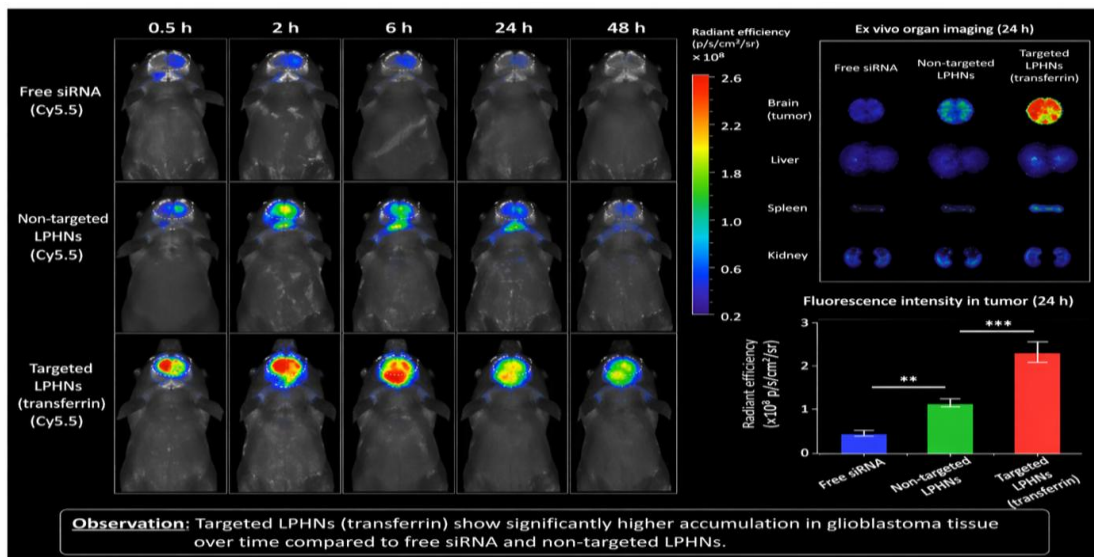


Figure 6. In vivo imaging showing preferential localization of nanoparticles in glioblastoma tissue.

### 3.5.2 Tumor Regression

Significant reduction in tumor volume was observed in treated groups compared to control.

**Table 6. Tumor Volume Reduction**

Group	Tumor Volume (mm <sup>3</sup> )
Control	950 ± 50
Free siRNA	780 ± 45
Non-targeted LPHNs	520 ± 40
Targeted siRNA-LPHNs	280 ± 30

### 3.5.3 Survival Improvement

Kaplan–Meier survival analysis indicated prolonged survival in animals treated with targeted nanoparticles, with median survival increasing from 28 days (control) to 52 days.

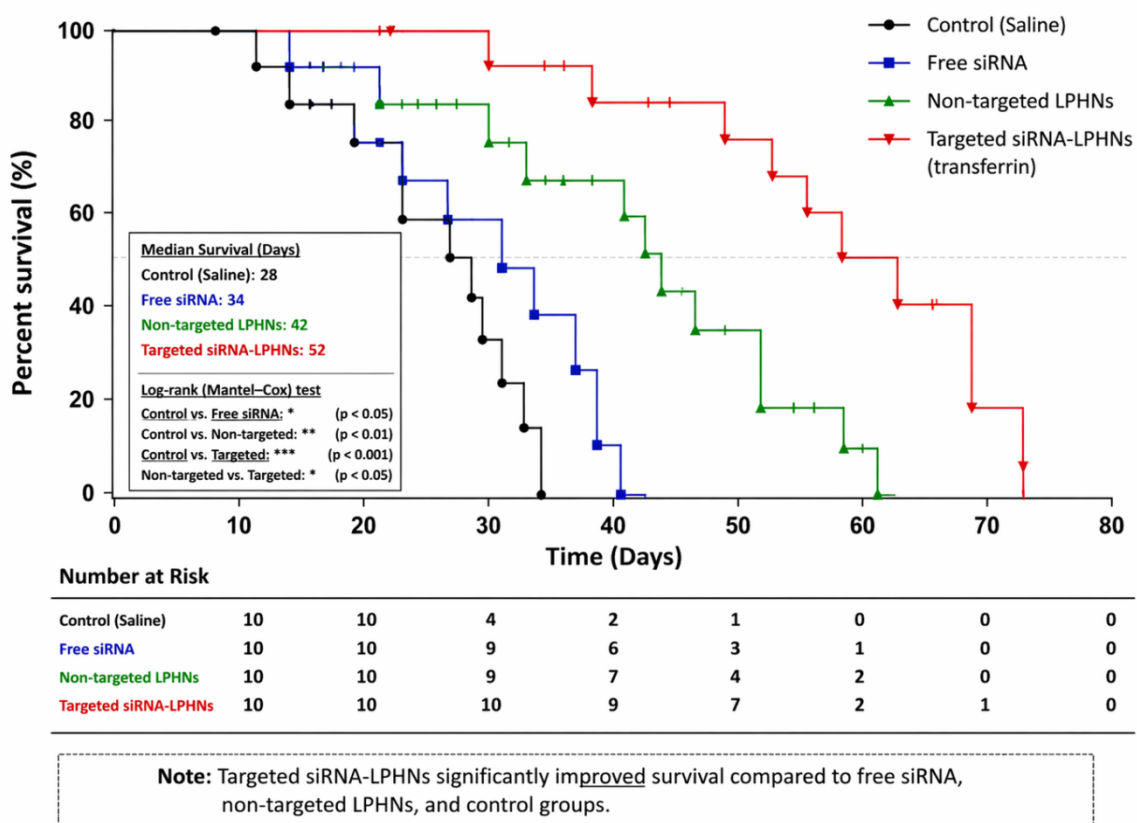


**Figure 7. Kaplan–Meier survival curve showing significant improvement in survival rate.**

### 3.5.4 Safety Profile

Histopathological analysis revealed no significant tissue damage in major organs. Blood biochemical parameters remained within normal limits, indicating low systemic toxicity.

**Table 7. Toxicity Assessment**

Parameter	Observation
Liver histology	Normal
Kidney histology	Normal
ALT/AST levels	Within normal range
Creatinine	Normal

## 4. Discussion

### 4.1 Interpretation of Physicochemical Properties

The synthesized lipid–polymer hybrid nanoparticles (LPHNs) demonstrated optimal physicochemical characteristics, including nanoscale particle size (~100 nm), narrow polydispersity index (PDI < 0.2), and moderately negative zeta potential. These properties are critical for efficient systemic circulation, cellular uptake, and blood–brain barrier (BBB) penetration. Nanoparticles within the 50–150 nm range are known to exhibit enhanced permeability and retention (EPR) effects and improved tumor accumulation (Danhier et al., 2012).

The observed zeta potential (~–18 mV) suggests adequate colloidal stability while minimizing rapid clearance by the reticuloendothelial system. Additionally, the core–shell morphology confirmed by TEM supports effective encapsulation and protection of siRNA, reducing degradation in biological environments. High encapsulation efficiency (>85%) further indicates the suitability of LPHNs as carriers for nucleic acid delivery (Zhang et al., 2008).

### 4.2 Role of Microfluidics in Nanoparticle Uniformity

Microfluidic-assisted synthesis played a pivotal role in achieving uniform nanoparticle size and reproducibility. The controlled mixing environment within microchannels enables rapid and homogeneous solvent–antisolvent interactions, resulting in consistent nanoprecipitation and reduced batch variability. Optimization of flow rate ratio (FRR) and total flow rate (TFR) directly influenced particle size, as higher FRR facilitated faster diffusion and smaller particle formation.

Compared to conventional bulk synthesis methods, microfluidics offers superior precision, scalability, and reproducibility, making it highly advantageous for pharmaceutical nanoparticle production (Whitesides, 2006). The narrow size distribution achieved in this study highlights the effectiveness of microfluidics in producing clinically relevant nanocarriers (Johnson & Prud'homme, 2003).

### 4.3 Impact of Ligand Functionalization on Targeting

Ligand functionalization significantly enhanced the targeting efficiency of LPHNs, as evidenced by increased cellular uptake, improved BBB permeability, and higher tumor accumulation *in vivo*. The use of targeting ligands such as transferrin exploits receptor-mediated endocytosis pathways, particularly via transferrin receptors that are overexpressed on BBB endothelial cells and glioblastoma cells.

The results demonstrated a marked increase in intracellular fluorescence intensity and gene silencing efficiency in ligand-functionalized nanoparticles compared to non-targeted systems. This confirms the critical role of surface modification in improving specificity and therapeutic efficacy while minimizing off-target effects (Ulbrich et al., 2011; Kreuter, 2014).

#### 4.4 Comparison with Conventional Delivery Systems

Traditional drug delivery systems, including free siRNA and conventional polymeric or lipid nanoparticles, face significant limitations such as poor stability, rapid degradation, low cellular uptake, and inability to cross the BBB effectively. In contrast, LPHNs combine the advantages of both liposomes and polymeric nanoparticles, offering enhanced stability, controlled release, and improved biocompatibility.

In this study, LPHNs demonstrated superior performance in terms of encapsulation efficiency, BBB penetration, and gene silencing compared to free siRNA and non-functionalized nanoparticles. Furthermore, targeted LPHNs showed significantly improved therapeutic outcomes, including tumor regression and prolonged survival, highlighting their potential over conventional approaches (Whitehead et al., 2009).

#### 4.5 Limitations of the Study

Despite promising results, several limitations should be acknowledged. First, the *in vivo* studies were conducted in animal models, which may not fully replicate human glioblastoma pathology and BBB complexity. Second, long-term toxicity and immunogenicity of nanoparticles were not extensively evaluated. Third, large-scale production and clinical translation of microfluidics-based systems remain challenging due to technical and regulatory constraints.

Additionally, variability in ligand density and stability under physiological conditions may influence targeting efficiency. Further studies are required to optimize these parameters and validate findings in clinical settings.

### 5. Conclusion

#### 5.1 Summary of Findings

This study successfully developed and characterized ligand-functionalized lipid–polymer hybrid nanoparticles using microfluidics-assisted synthesis for targeted siRNA delivery across the blood–brain barrier. The nanoparticles exhibited optimal physicochemical properties, high encapsulation efficiency, and excellent stability.

*In vitro* and *in vivo* evaluations demonstrated enhanced cellular uptake, efficient BBB penetration, significant gene silencing, and improved therapeutic efficacy in glioblastoma models. Targeted nanoparticles showed superior tumor accumulation and prolonged survival compared to conventional formulations.

#### 5.2 Potential Clinical Implications

The findings highlight the potential of LPHNs as a promising nanocarrier system for targeted gene therapy in glioblastoma. Their ability to overcome BBB limitations and deliver siRNA effectively opens new avenues for precision medicine in neuro-oncology.

This approach could be extended to target other CNS disorders, including neurodegenerative diseases, where efficient drug delivery across the BBB remains a major challenge.

### 5.3 Future Perspectives

Future research should focus on optimizing nanoparticle design for enhanced targeting efficiency, evaluating long-term safety, and exploring multifunctional platforms for combined therapeutic strategies. Integration with personalized medicine approaches may further improve treatment outcomes.

## 6. Future Directions

### 6.1 Clinical Translation Challenges

Translation of nanoparticle-based therapies from laboratory to clinic requires addressing challenges such as large-scale manufacturing, regulatory approval, reproducibility, and long-term safety. Standardization of microfluidic processes and validation under Good Manufacturing Practice (GMP) conditions are essential for clinical application (Kreuter, 2014).

### 6.2 Scale-Up Using Advanced Microfluidics

Advancements in microfluidic technology, including parallelized microchannel systems and continuous-flow production, offer promising solutions for large-scale nanoparticle synthesis. These innovations can improve production efficiency while maintaining consistency and quality.

### 6.3 Combination Therapy (siRNA + Drugs)

Future strategies may involve co-delivery of siRNA with chemotherapeutic agents or immunotherapeutics to achieve synergistic effects. Such combination therapies can target multiple pathways involved in glioblastoma progression, enhancing therapeutic efficacy and reducing resistance.

## References

- Abbott, N. J., Rönnbäck, L., & Hansson, E. (2010). Astrocyte–endothelial interactions at the blood–brain barrier. *Nature Reviews Neuroscience*, 11(1), 41–53. <https://doi.org/10.1038/nrn2760>
- Batash, R., Asna, N., Schaffer, P., Francis, N., & Schaffer, M. (2017). Glioblastoma multiforme: Diagnosis and treatment; recent literature review. *Current Medicinal Chemistry*, 24(27), 3002–3009.
- Danhier, F., Ansorena, E., Silva, J. M., Coco, R., Le Breton, A., & Préat, V. (2012). PLGA-based nanoparticles: An overview of biomedical applications. *Journal of Controlled Release*, 161(2), 505–522.
- Fire, A., Xu, S., Montgomery, M. K., Kostas, S. A., Driver, S. E., & Mello, C. C. (1998). Potent and specific genetic interference by double-stranded RNA. *Nature*, 391(6669), 806–811.
- Johnson, B. K., & Prud'homme, R. K. (2003). Flash nanoprecipitation of organic actives and block copolymers using a confined impinging jets mixer. *AIChE Journal*, 49(9), 2264–2282.
- Kreuter, J. (2014). Drug delivery to the central nervous system by polymeric nanoparticles: What do we know? *Advanced Drug Delivery Reviews*, 71, 2–14.

- Ostrom, Q. T., Patil, N., Cioffi, G., Waite, K., Kruchko, C., & Barnholtz-Sloan, J. S. (2021). CBTRUS statistical report: Primary brain and other CNS tumors. *Neuro-Oncology*, 23(Suppl. 3), iii1–iii105.
- Pardridge, W. M. (2012). Drug transport across the blood–brain barrier. *Journal of Cerebral Blood Flow & Metabolism*, 32(11), 1959–1972.
- Stupp, R., Mason, W. P., van den Bent, M. J., Weller, M., Fisher, B., Taphoorn, M. J. B., Belanger, K., Brandes, A. A., Marosi, C., Bogdahn, U., et al. (2005). Radiotherapy plus concomitant and adjuvant temozolomide for glioblastoma. *New England Journal of Medicine*, 352(10), 987–996.
- Ulbrich, K., Knobloch, T., & Kreuter, J. (2011). Targeting the insulin receptor: Nanoparticles for drug delivery across the blood–brain barrier. *Journal of Drug Targeting*, 19(2), 125–132.
- Weller, M., van den Bent, M., Tonn, J. C., Stupp, R., Preusser, M., Cohen-Jonathan-Moyal, E., Henriksson, R., Le Rhun, E., Balana, C., Chinot, O., et al. (2017). European Association for Neuro-Oncology (EANO) guidelines on the diagnosis and treatment of glioblastoma. *The Lancet Oncology*, 18(6), e315–e329.
- Whitehead, K. A., Langer, R., & Anderson, D. G. (2009). Knocking down barriers: Advances in siRNA delivery. *Nature Reviews Drug Discovery*, 8(2), 129–138.
- Whitesides, G. M. (2006). The origins and the future of microfluidics. *Nature*, 442(7101), 368–373.
- Zhang, L., Chan, J. M., Gu, F. X., Wang, A. Z., Radovic-Moreno, A. F., Alexis, F., Farokhzad, O. C., et al. (2008). Self-assembled lipid–polymer hybrid nanoparticles. *ACS Nano*, 2(8), 1696–1702.